







































































































































































































### 4.4.3 High resolution scanning electron microscopy (HRSEM)

The scanning electron microscopy shows the morphology of continuous Pd layer deposited onto Ti6Al4V substrate, as illustrated in Figure 4.23. The depth of electrons was calculated using the following expression:

$$R = \frac{4120}{\rho} \times E^{(1.265-0.0954 \ln E)} \quad [4.17] \quad (4.1)$$

where R is the depth of electrons in microns, E is the primary electron energy in MeV and  $\rho$  is the density of Pd in  $\frac{g}{cm^3}$ . The penetration of electrons in Pd layer was determined to be approximately 30 nm at 5 keV.

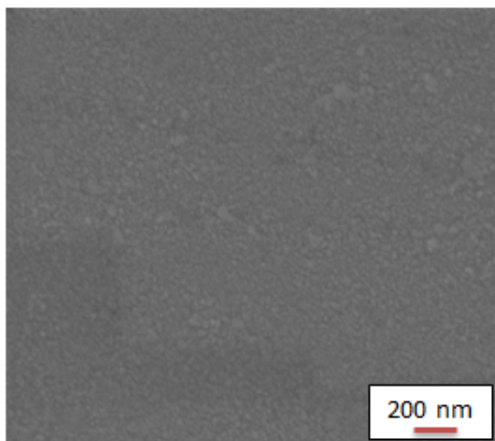


Figure 4.23: SEM micrograph of Pd coated layer (thickness of 200 nm) deposited on Ti6Al4V alloy substrate.

SEM images of Pd coated Ti6Al4V alloy after hydrogenation at different temperature are presented in Figure 4.24. The coating morphology of the sample hydrogenated at room temperature (Figure 4.24A) is not changed significantly in comparison to its as-deposited morphology (Figure 4.23) while the significant changes occurred in the samples hydrogenated at elevated temperatures. At 450 °C (Figure 4.24B), the coating became discontinuous indicating the consumption of Pd by reaction with substrate material and possible reaction with hydrogen. The formation of islands and cubic like structures were observed after hydrogenation at 550 °C (Figure 4.24C). After hydrogenation at even higher temperature (650 °C/ 3 hours), the coating morphology showed smoother appearance probably due to growth of cubic crystals (Figure 4.24D).

In order to understand the changes in coating morphology, the RBS and XRD measurements were performed.

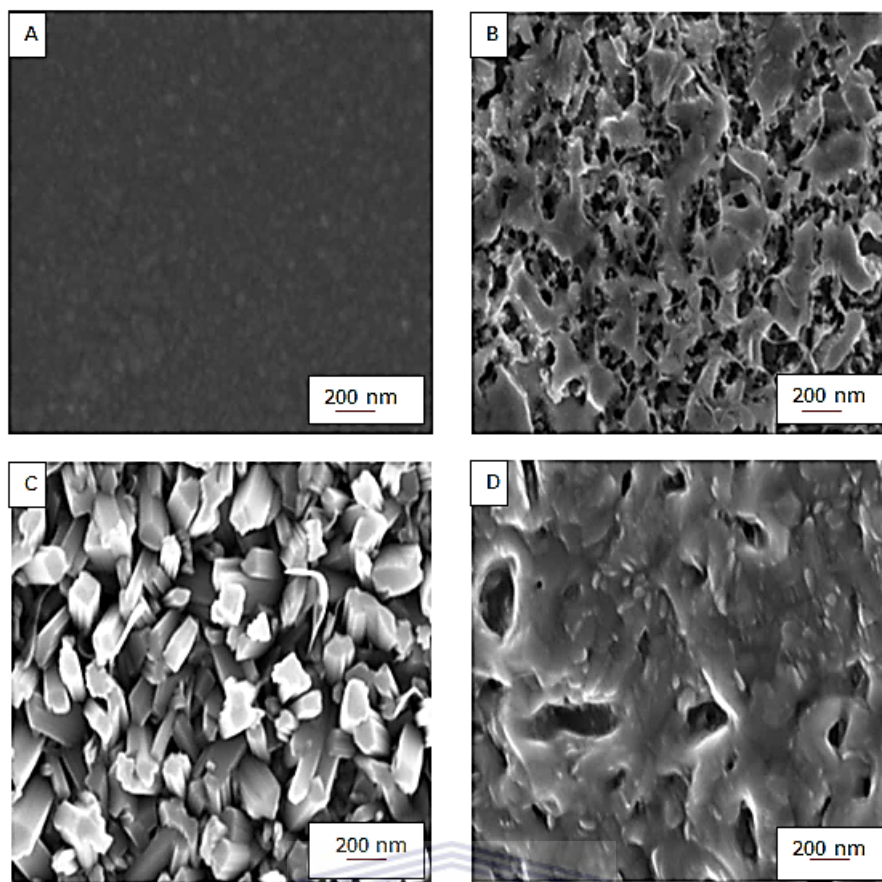


Figure 4.24: Morphology of Pd/Ti6Al4V system hydrogenated at room temperature, 450 °C, 550 °C and 650 °C for a period of 3 hours.

#### 4.4.4 Rutherford Backscattering Spectrometry

RBS was used to determine the changes in Pd coating thickness and its stoichiometry caused by high temperature hydrogenation process. Experimental and simulated RBS spectra of Pd/Ti6Al4V system, Figure 4.25, shows the thickness of Pd layer of 204 nm which is in good agreement with thickness measured by quartz crystal (201 nm). The RBS results also show that no reaction occurred during coating deposition of Pd on Ti6Al4V substrate. The thickness of Pd layer deposited on Ti6Al4V alloy was approximately 200 nm in all samples used in this study.

Figure 4.26 shows RBS spectra of Pd coated Ti6Al4V alloy after hydrogenation. There is no significant change in the RBS spectra of Pd/Ti6Al4V hydrogenated at room temperature and 450 °C in comparison to the as-deposited sample (Figure 4.25). As opposed to the RBS spectrum of uncoated Ti6Al4V alloy, the oxygen peak was not detected after hydrogenation at 450 °C. This shows Pd layer protected the Ti6Al4V alloy against oxidation at 450 °C. After hydrogenation at 550 °C and 650 °C there was a significant change in the RBS spectrum due to reaction between coating and substrate materials.

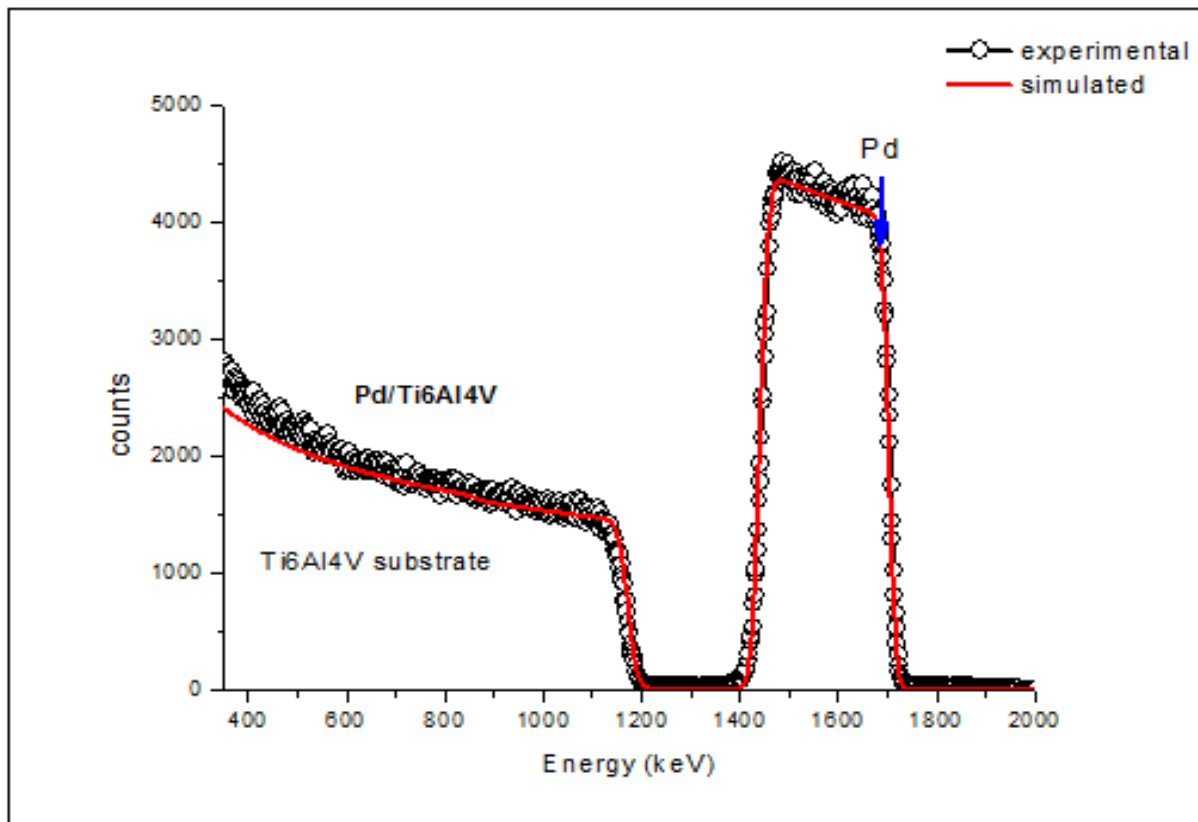


Figure 4.25: RBS spectra Pd film with thickness of 200 nm deposited on Ti6Al4V, the arrow indicate Pd edge.

The RBS spectrum of Pd/Ti6Al4V alloy after hydrogenation at 550 °C can be divided into 3 regions, the first region (1) is the near surface region only a small amount of Pd was detected (2.51 at.%). In region 2 concentration of Pd increased to 11.75 at.% and then decreased (region 3) where the concentration of Pd was 3.55 at.%. Similarly RBS spectra of the sample hydrogenated at 650 °C can be divided into three different regions, on the surface (region 1) amount of Pd detected was 1.43 at.%, in region 2 about 3 at.% of Pd was detected. In region 3 concentration of Pd increased to 17.58 at.%. In addition, the oxygen peak was observed in the sample hydrogenated at 650 °C.

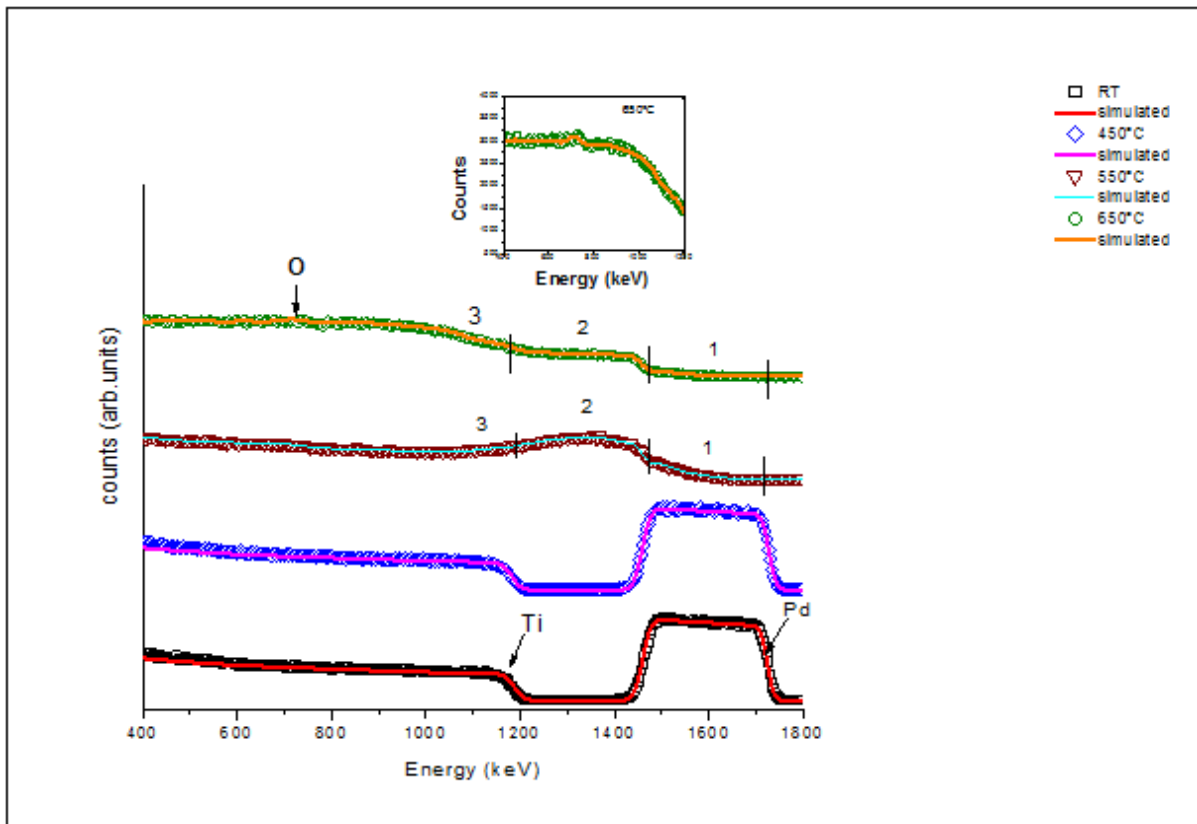


Figure 4.26: RBS spectra showing Pd coated Ti6Al4V alloy after hydrogenation at room temperature, 450 °C, 550 °C and 650 °C. The numbers indicate the regions relative to Pd concentration.

In summary, the variation in Pd concentration after hydrogenation at 550 °C and 650 °C indicate diffusion of Pd into the substrate material. In order to investigate the formation of phases, the X-ray diffraction experiments were performed.

#### 4.4.5 X-ray diffraction

The X-ray diffraction of Pd/Ti6Al4V before hydrogenation (as deposited) and after hydrogenation at different temperature is shown in Figure 4.27. Palladium peaks and  $\alpha$ -Ti peaks in the as deposited samples are observed as expected. After hydrogenation at room temperature the XRD pattern remained unchanged. At 450 °C in addition to the Pd and Ti peaks, the hydride peaks were identified,  $\text{TiH}_2$  and  $\text{TiH}_{1.924}$ . It was also observed that the peaks shifted to lower diffraction angles indicating the presence of compressed stress in the material. When hydrogen is absorbed into the material, the formation of hydrides induces stress at the grain boundaries [4.18]. XRD pattern of Pd/Ti6Al4V after hydrogenation at 550 °C shows the presence of  $\alpha$ -Ti,  $\text{TiH}_2$ ,  $\text{Pd}_3\text{Ti}$  and  $\text{Pd}_5\text{Ti}_3$  phases. The Pd peaks were not observed at 550 °C and 650 °C and it is an indication that Pd was consumed by reaction with substrate material. This result is in agreement with RBS

results which showed diffusion of Pd into the Ti6Al4V substrate. XRD pattern of the sample hydrogenated at 650 °C exhibited peaks corresponding to TiO,  $\alpha$ -Ti and Ti<sub>2</sub>Pd<sub>3</sub>. In addition, at high temperatures (550 °C and 650 °C) XRD pattern shows evidence of reaction between Pd and Ti which lead to the formation of Pd<sub>3</sub>Ti and Pd<sub>5</sub>Ti<sub>3</sub> at 550 °C and Ti<sub>2</sub>Pd<sub>3</sub> at 650 °C.

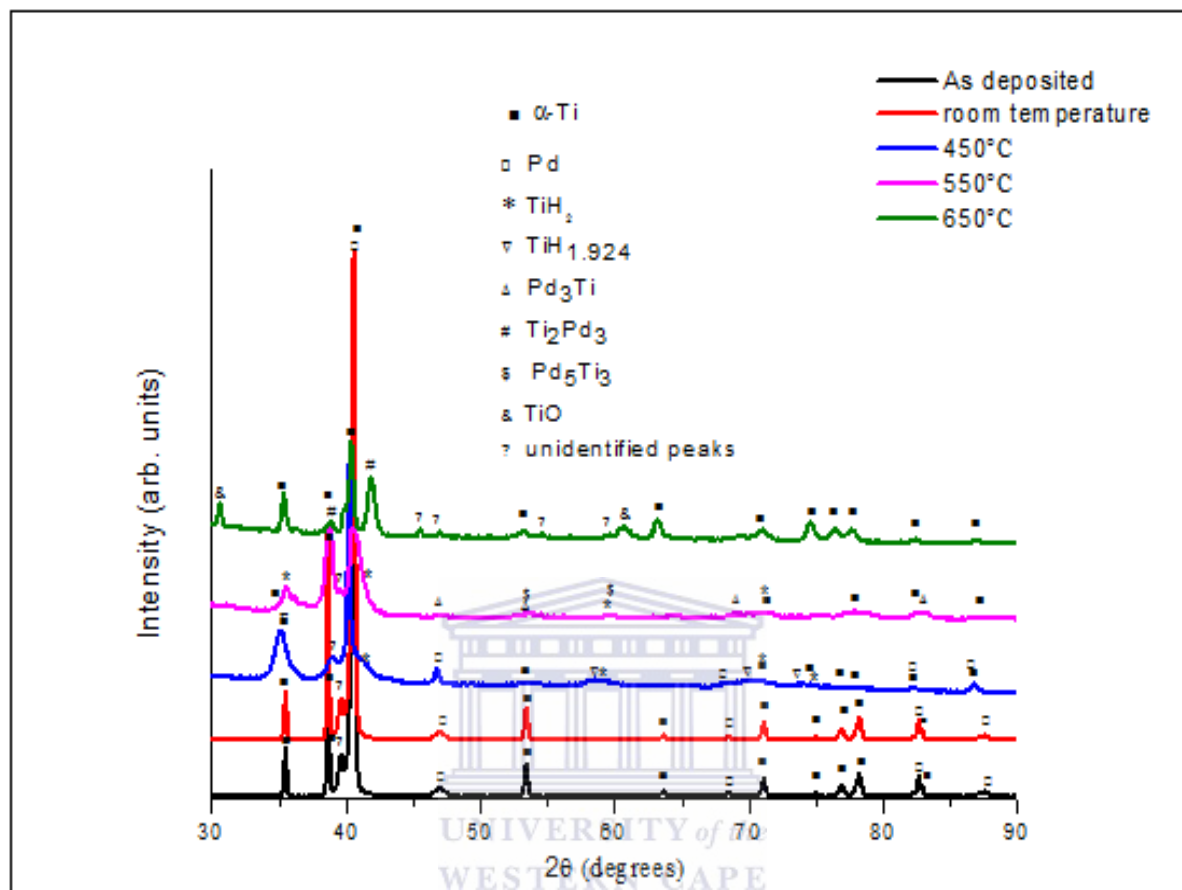


Figure 4.27: XRD patterns of Pd/Ti6Al4V before hydrogenation and after hydrogenation at room temperature, 450 °C, 550 °C and 650 °C.

In summary XRD results indicate that hydrogenation at 450 °C and 550 °C leads to formation of titanium hydrides. At room temperature and higher temperature of 650 °C hydride formation did not take place. After hydrogenation at high temperatures, alloying of Pd layer with Ti in the form of Pd<sub>5</sub>Ti<sub>3</sub>, Pd<sub>3</sub>Ti at 550 °C and in the form of Ti<sub>2</sub>Pd<sub>3</sub> at 650 °C was observed.

#### 4.4.6 Discussions of results on Pd coated Ti6Al4V alloy

In the previous section it was shown that significant hydrogen uptake in CP-Ti and Ti6Al4V alloy begins at temperatures of 550 °C. No significant amount of hydrogen was observed at temperatures below 550 °C. The metal surface of the hydrogen storage materials needs to be activated

before they can absorb hydrogen. This can be achieved by hydrogenating at high temperature and pressure or by coating the surface with a catalytic layer. In this work Ti6Al4V alloy samples were coated with thin layer of Pd. The hydrogen storage capacity of Pd/Ti6Al4V at different temperatures was investigated using ERDA. The results showed that concentration of hydrogen in Pd/Ti6Al4V alloy is temperature dependent. The concentration increases with increasing temperature up to 550 °C and decreases at high temperatures (650 °C). The hydrogen absorption trend in Pd coated Ti6Al4V alloy samples is similar to that of uncoated Ti6Al4V but the difference is in the amount of hydrogen absorbed. The hydrogen storage capacity of Pd coated and uncoated Ti6Al4V alloy at different temperatures were compared in Table 4.7 (page 79). It was found that Pd coated Ti6Al4V alloy absorbs more hydrogen than the uncoated Ti6Al4V alloy samples. It can be concluded hydrogen Pd layer improved the hydrogen storage capacity of Ti6Al4V alloy. Significant hydrogen absorption took place at lower temperature (450 °C) in Pd coated Ti6Al4V alloy in comparison to the uncoated Ti6Al4V alloy samples. This shows that Pd layer lowers hydrogen absorption start temperature in Ti. These observations agree with the observations of Shugard et al [4.19]. The authors showed that 180 nm Pd layer deposited on Ti allows hydrogen absorption at low temperatures. The maximum depth of hydrogen diffusion in Pd/Ti6Al4V alloy was greater than that of Ti6Al4V. Pd promotes dissociation of hydrogen molecules onto the Ti surface and hydrogen atoms diffuse easily in the bulk of the metal.

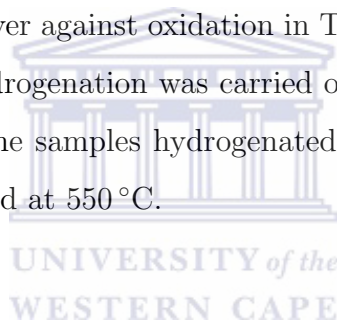
According to RBS results the oxygen peak was not detected in Pd/Ti6Al4V alloy samples hydrogenated at room temperature, 450 °C and 550 °C. It should be noted that in the uncoated Ti6Al4V alloy thick oxide layer was formed after hydrogenation at 450 °C and 550 °C. This implies that Pd protected Ti6Al4V alloy samples against oxidation during hydrogenation at 450 °C and 550 °C. At 650 °C Ti6Al4V alloy was oxidized. Heller et al [4.20] reported on the effect of Pd as a protective layer against oxidation, and it was shown that with increase in temperature thicker layer is required to prevent oxidation of Ti. It can be concluded that at 200 nm layer was not thick enough to prevent surface oxidation in Ti6Al4V alloy hydrogenated at 650 °C.

After hydrogenation at room temperature no hydride formation occurred. TiH<sub>2</sub> were formed at 450 °C and 550 °C. Pd coating lowered hydride formation temperature in Ti6Al4V alloy to 450 °C, which was 550 °C in the case of uncoated Ti6Al4V. alloy. Hydrogenation at high temperatures of 650 °C, did not lead to formation of hydrides. High temperature hydrogenation caused Pd layer to diffuse into the Ti6Al4V alloy substrate, as a result Pd<sub>3</sub>Ti and Pd<sub>5</sub>Ti<sub>3</sub> at 550 °C and

Ti<sub>2</sub>Pd<sub>3</sub> at 650 °C were formed.

#### 4.4.7 Conclusion

It was observed that hydrogen absorption in Pd/Ti6Al4V alloy samples is temperature dependent. The amount of hydrogen increased with increasing temperature up to 550 °C and decreased at higher temperature of 650 °C. At room temperature Pd protects the surface against oxidation and dissociates hydrogen atoms into the surface. Generally at high temperatures Pd protects the surface against oxidation and Pd is incorporated on Ti, forming different phases. The increase in hydrogen at 450 °C and 550 °C is caused by formation of hydrides, whereas at the concentration of hydrogen decreased and hydrides are not formed. Comparing Ti6Al4V alloys with and without Pd coating on the surface, it shows significantly that low hydrogen content was absorbed, indicating the effect of Pd on dissociation of hydrogen. The maximum amount of hydrogen (36.71 at.%) was absorbed at 550 °C. Increased hydrogen storage capacity and lower hydride formation start temperature was found in Pd coated alloy in comparison to the uncoated Ti6Al4V alloy samples. Pd layer also acts as a protective layer against oxidation in Ti6Al4V alloy. Hydride formation did not occur in Pd/Ti6Al4V when hydrogenation was carried out at room temperature and 650 °C. TiH<sub>1.92</sub> and TiH<sub>2</sub> were formed in the samples hydrogenated at 450 °C, while only the TiH<sub>2</sub> was observed in the sample hydrogenated at 550 °C.



# References

- [4.1] B. Fenf, J. Wrng, B.C. Yang, J.Y. Chen, J.Z. Zhao, L. He, S.K. Qi, X.D. Zhang, Surface characterization of titanium and adsorption of bovine serum albumin, *Materials Characterization*, **49**, 129-137 (2003).
- [4.2] E. Gemelli, N.H.A. Camargo, Oxidation kinetics of commercially pure titanium, *Revista Matéria*, **12**, 525-531 (2007).
- [4.3] D. Velten, V. Biehl, F. Aubertin, B. Valeske, W. Possart, J. Breme, Preparation of TiO<sub>2</sub> layers on CP-Ti and Ti6Al4V by thermal and anodic oxidation and by sol-gel coating techniques and their characterization, *Journal of Biomedical Materials Research*, **59**, 18-28 (2002).
- [4.4] T. Yoneyama, S. Mayazaki, Editors, *Shape memory alloys for biomedical applications*, Woodhead Publishing Limited (2009).
- [4.5] J.C. Rivière, S. Myhra, Editors, *Handbook of surface and interface analysis: methods for problem-solving*, CRC press (2009).
- [4.6] A. San-Martin, F.D. Manchester, The H-Ti (Hydrogen-Titanium) system, *Bulletin of Alloy Phase Diagrams*, **8**, 30-42 (1987).
- [4.7] D.B. Shan, Y.Y. Zong, T.F. Lu, Y. Lv, Microstructural evolution and formation mechanism of FCC titanium hydride in Ti-6Al-4V-xH alloys, *Journal of Alloys and Compounds*, **427**, 229-234 (2007).
- [4.8] Y. Zhang, S.Q. Zhang, Hydrogenation Characteristics of Ti-6Al4V cast alloy and its microstructural modification by hydrogen treatment, *International Journal of Hydrogen Energy*, **22**, 161-168 (1997).

- [4.9] A. Lopez-Suarez, J. Rickards, R. Trejo-Luna, Analysis of hydrogen absorption by Ti and Ti-6Al-4V using the ERDA technique, *International Journal of Hydrogen Energy*, **28**, 1107-1113 (2003).
- [4.10] A. Murzinova, Effect of hydrogen on microstructure of  $\alpha$ -Ti alloys deformed at 600 °C, *Letters on Materials*, **4**, 214-217 (2014).
- [4.11] S. Markelj, I. Čadež, P. Pelicon and Z. Rupnik, Studying processes of hydrogen interaction with metallic surfaces in situ and in real-time by ERDA, *Nuclear Instruments and Methods in Physics Research Section B: Beam Interactions with Materials and Atoms*, **259**, 989-996 (2007).
- [4.12] F.X. Gil, D. Rodriguez, J.A. Planell, Grain growth kinetics of pure titanium, *Scripta Metallurgica et Materialia*, **33**, 1361-1366 (1995).
- [4.13] T. Zhu, M. Li, Effect of 0.770 wt % H addition on the microstructure of Ti-6Al-4V alloy and mechanism of  $\sigma$ -hydride formation, *Journal of Alloys and Compounds*, **481**, 480-485 (2009).
- [4.14] J.I. Qazi, and O.N. Senkov, F.H. Froes, Phase transformations in the Ti-6Al-4V-H system, *The Journal of The Minerals, Metals and Materials Society*, **54**, 68 - 71 (2002).
- [4.15] F.H. Froes, O.N. Senkov, J.I Qazi, Hydrogen as a temporary alloying element in titanium alloys : thermohydrogen processing, *International Materials Reviews*, **49**, 227-245 (2004),
- [4.16] H.J. Liu, L. Zhou, P. Liu, Q.W. Liu, Microstructural evolution and hydride precipitation mechanism in hydrogenated Ti-6Al-4V alloy, *International Journal of Hydrogen Energy*, **34**, 9596 – 9602 (2009).
- [4.17] P.J. Goodhew, F.J. Humphreys, *Electron microscopy and analysis*, Taylor and Francis (1988).
- [4.18] A. López-Suárez, Influence of surface roughness on consecutively hydrogen absorption cycles in Ti-6Al-4V alloy, *International Journal of Hydrogen Energy*, **35**, 10404-10411 (2010).
- [4.19] A.D. Shugard, R.T. Walters, P.V. Blarigan, Titanium tritide radioisotope heat source development: Palladium-coated titanium hydriding kinetics and tritium loading tests, *Energy Conversion and Management*, **64**, 371-377 (2012).

- [4.20] E.M.B. Heller, J.F. Suyver, A.M. Vredenberg, D.O. Boerma, Oxidation and annealing of thin FeTi layers covered with Pd, *Applied Surface Science*, **150**, 227-234 (1999).



# Chapter 5

## Conclusions

The aim and the scope of this work were to investigate the hydrogen storage capacity of CP-Ti, Ti6Al4V alloy and Pd coated Ti6Al4V alloy (Pd/Ti6Al4V), the effects of hydrogen on the microstructure and phase transformation. Hydrogenation was carried out in a vacuum furnace under 15% H/ Ar atmosphere at a pressure of 1 bar. Samples were hydrogenated at room temperature, 450 °C, 550 °C and 650 °C each for a period of 3 hours. The concentration of hydrogen in Ti6Al4V alloy and Pd/Ti6Al4V alloy were compared to understand the effect of Pd on hydrogen storage capacity of Ti6Al4V alloy. ERDA and gravimetric method were used to determine their hydrogen storage capacity. The surface composition, the microstructure and phase analysis were studied using RBS, optical microscope, scanning electron microscopy and X-ray diffraction, respectively. The results obtained from this study were presented and discussed in chapter 4 and the following conclusions were drawn for each material under investigation:

### 5.1 CP-Ti

RBS results showed that the samples were oxidized during hydrogenation at 450 °C, 550 °C and 650 °C leading to the formation of TiO<sub>2</sub> layer with thickness of 60 nm. ERDA and gravimetric method showed that hydrogen absorption depends on hydrogenation temperature. A huge amount of hydrogen was absorbed at 550 °C (45.65 at.%H ) and it decreased to 37.53 at.%H at 650 °C as determined by ERDA. Hydrogen absorption leads to formation of hydrides (in some cases results show formation of TiH<sub>2</sub>) in samples hydrogenated at 550 °C and 650 °C. No hydride formation occurred in the samples hydrogenated at room temperature and 450 °C. The optical microscopy results showed that at high hydrogenation temperatures (550 °C and 650 °C), the needle-like martensite structure was formed. Comparison was made with microstructures of

as-received and annealed samples. The microstructure of as-received samples was composed of equiaxed alpha grains which increased with increasing temperature; at 550 °C the grain size was 103  $\mu\text{m}$  and increased to 108  $\mu\text{m}$  at 650 °C.

## 5.2 Ti6Al4V alloy

Similar to CP-Ti significant hydrogen absorption began at 550 °C, and average hydrogen concentration was 34.77 at.%. After hydrogenation at 650 °C the concentration of hydrogen decreased. Hydrogen absorption at 550 °C and 650 °C caused formation of fine and course needle-like structures, respectively. Titanium hydrides were not detected in the samples hydrogenated at room temperature, 450 °C and 650 °C, however formation of  $\text{TiH}_2$  was observed at 550 °C.

## 5.3 Pd/Ti6Al4V system

In Pd/Ti6Al4V significant hydrogen absorption began at lower temperatures (450 °C) as compared to Ti6Al4V alloy. The amount of hydrogen increased at 450 °C and 550 °C and decreased to 650 °C. At 450 °C the amount of hydrogen absorbed was 30.24 at.% and increased to 36.70 at.% H at 550 °C and decreased to 25.65 at.%H at 650 °C. It is shown that Pd enhances hydrogen increases hydrogen concentration in Ti6Al4V alloy and act as a protective layer against oxidation. It was found that Pd coated Ti6Al4V alloy absorbs more hydrogen than the uncoated Ti6Al4V alloy.  $\text{TiH}_2$  phase were formed after hydrogenation at 450 °C and 550 °C. No hydride phase were detected by XRD in the samples hydrogenated at room temperature and 650 °C. Ti-Pd intermetallic phases were formed in the samples hydrogenated at 550 °C and 650 °C.  $\text{PdTi}_3$  and  $\text{Pd}_5\text{Ti}_3$  phases were observed at 550 °C, whereas  $\text{Ti}_2\text{Pd}_3$  phase was formed at 650 °C.

Scanning electron microscopy showed that room temperature hydrogenation does not affect the coating morphology, while at high hydrogenation temperatures the morphology changed significantly. Cubic-like structures and small "islands" formed in the sample hydrogenated at 550 °C.

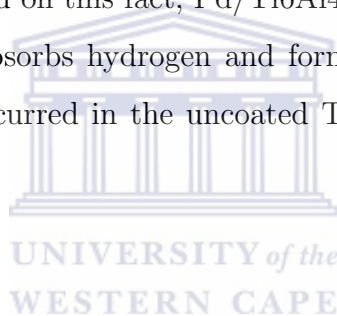
## 5.4 General conclusion

The hydrogen storage capacity of the three different systems is summarised in Table 5.1.

Table 5.1: Comparison of hydrogen storage capacity in CP-Ti, Ti6Al4V and Pd/Ti6Al4V

	CP-Ti	Ti6Al4V	Pd/Ti6Al4V
Temperature (°C)	at%H	at.%H	at%H
RT	0.19	1.01	4.76
450	0.25	1.12	30.24
550	45.65	34.77	36.70
650	37.53	3.67	25.65

In general, the comparison between the three types of materials investigated in study shows that CP-Ti absorbs more hydrogen than Pd/Ti6Al4V and Ti6Al4V alloy at high temperatures (550 °C and 650 °C). However for energy storage applications it is best for hydrogen to be absorbed at lower temperatures. Therefore based on this fact, Pd/Ti6Al4V alloy system is the best candidate for hydrogen storage, because it absorbs hydrogen and forms hydrides at lower temperature of 450 °C (no hydrogen absorption occurred in the uncoated Ti6Al4V alloy and CP-Ti samples at temperatures below 550 °C).



# Appendix A

## Thickness conversion from monolayers to nm

For  $\text{TiO}_2$  layer with thickness of  $600 \times 10^{15}$  atoms/cm<sup>2</sup> with a density of 4.23 g/cm<sup>3</sup>.

First find the atomic density:

$$\rho_{\text{atomic}} = \frac{\rho_{\text{mass}}(\text{g/cm}^3) \times N(\text{atoms/mol}) \times a(\text{a.u})}{M_r} \quad (\text{A.1})$$

Avogadro's number  $N = 6.022 \times 10^{23}$  atoms/mol, number of atoms  $a = 1 + 2 = 3$ , molar mass  $M_r = 79.866$  g/mol

$$\rho_{\text{atomic}} = \frac{(4.23 \text{g/cm}^3)(3)(N = 6.022 \times 10^{23} \text{ atoms/mol})}{79.866 \text{ g/mol}} \quad (\text{A.2})$$

$$= 9.57 \times 10^{22} \text{ atoms/cm}^3 \quad (\text{A.3})$$

secondly find thickness  $Th$  in cm

$$Th(\text{cm}) = \frac{Th(\text{atoms/cm}^2)}{\rho_{\text{atomic}}} \quad (\text{A.4})$$

$$= \frac{600 \times 10^{15} \text{ atoms/cm}^2}{9.57 \times 10^{22} \text{ atoms/cm}^3} \quad (\text{A.5})$$

$$= 62.69 \times 10^{-7} \text{ cm} \quad (\text{A.6})$$

Finally convert from cm to nm :

$$Th(\text{nm}) = 62.69 \times 10^{-7} \text{ cm} \times 10^7 = 62.69 \text{ nm}$$

# Appendix B

## Detailed calculation for mass gain measurements

Suppose the mass before and after hydrogenation is  $m_1$  and  $m_2$ , respectively. The change in mass after hydrogenation is given by  $m_2 - m_1$ . As an example, for the Ti6Al4V alloy sample hydrogenated at 550,  $m_1 = 0.471$  g and  $m_2 = 0.478$  g

Table B.1: Formula used to calculate wt.% and at.% of hydrogen by gravimetric method

	Ti	Al	V	H
Molar Mass (g/mol)	47.87	26.98	50.94	1.01 (wt%)
Mass of elements (g)	$(m_1 * 0.9)$	$(m_1 * 0.06)$	$(m_1 * 0.04)$	$m_2 - m_1$
$\text{wt.\%} = (\text{row 3} / \text{sum of row 3}) * 100$	87.5	6.25	4.16	2.08
$\frac{\text{wt.\%}}{\text{MolarMass}}$	1.83	0.23	0.08	2.06
$\text{at.\%} = (\text{row 4} / \text{sum of row 4}) * 100$	43.57	5.47	1.9	49.04

Table B.2: wt.% and at.% of hydrogen in Ti6Al4V alloy at different temperatures obtained by gravimetric method

Temperature	$m_1$	$m_2$	mass gain	wt.%	at.%
RT	0.8907	0.8910	0.0003	0.03	1.29
450	0.838	0.840	0.002	0.24	9.78
550	0.471	0.478	0.01	2.08	49.04
650	0.887	0.894	0.01	0.78	26.52

For CP-Ti hydrogenated at 550 °C, m1 = 0.844 and m2 = 0.858 g

Table B.3: Formula used to calculate wt.% and at.% of hydrogen in CP-Ti using mass gain

	Ti	H
Molar Mass (g/mol)	47.87	1.01 (wt%)
Mass of elements (g)	m1	m2-m1
wt.% = (row3/sum of row 3)*100	98.25	1.75
$\frac{wt.\%}{MolarMass}$	2.053	1.732
at.% = ( row 4/sum of row 4)*100	54.231	45.769

Table B.4: wt.% and at.% of hydrogen in CP-Ti at different temperatures obtained by gravimetric method

Temperature	m1	m2	mass gain	wt.%	at.%
RT	0.844	0.844	—	—	—
450	0.796	0.797	0.001	0.13	5.26
550	0.844	0.859	0.02	1.75	45.46
650	1.058	1.072	0.01	1.306	38.59

